energies

MDPI

Article

Solar Irradiance Stability Factors

Borut Jereb

Faculty of Logistics, University of Maribor, 3000 Celje, Slovenia; borut.jereb@um.si

Abstract: In the field of renewable energies, the logistical intricacies of production, as well as the use and storage of photovoltaic energy, have become critical issues. In addition to sheer quantity, the stability of this type of energy is a crucial factor in ensuring the reliability and consistency of power generation. This paper defines Solar Irradiance Stability Factors (*SISF*s) as indicators complementing electricity production. When planning solar energy production in each geographical area, both the quantity and stability of solar irradiance are necessary for exploitation and determining the quality of solar irradiance. While the average production of solar energy per unit area in each time interval is a widely used parameter in daily practice, the observation of the amplitude of solar irradiance and its influence on energy production in the observed time interval is currently still rare. The *SISF*s defined in this article are new metrics that mainly depend on the meteorological variability in an area, and the observed time intervals should be in the range of seconds, minutes, or even hours. Larger time intervals are not helpful for the stability of solar irradiance in energy production and logistics from the source to the destination. They provide a complementary and more accurate measure of how suitable a particular geographical area is for producing solar energy.

Keywords: solar irradiance; stability metrics; photovoltaic energy; meteorological variability; geographical area

Citation: Jereb, B. Solar Irradiance Stability Factors. *Energies* **2024**, *17*, 4549. https://doi.org/10.3390/en17184549

Academic Editors: Francesco Nocera and Xiaohu Yang

Received: 13 August 2024
Revised: 2 September 2024
Accepted: 9 September 2024
Published: 11 September 2024

1. Introduction

The electrical capacity for solar installations in 2019 was 700 times higher than in 2000 [1]. At the forefront of PV energy utilization and storage is the concept of the "electric energy warehouse" [2], where the effective management and storage of energy resources are critical to sustainable energy systems. In this warehouse, the effective management and storage of energy resources becomes not only a technological challenge but a must to realize the full potential of renewable energy.

The critical aspect of optimizing the amount of usable PV energy is an optimization and, therefore, a multi-faceted challenge involving the subtleties of solar irradiance, the efficiency of photovoltaic modules, and the influence of environmental conditions. The logistics of maximizing the amount of PV energy harvested [3] requires a comprehensive analysis that combines technological advances with environmental considerations.

The inherent variability of solar energy production, influenced by panel orientation, number of light hours per day, site solar irradiance, weather conditions, and system efficiency, requires a nuanced approach to ensure power generation reliability and consistency [4,5]. Dealing with the logistics of stability becomes a cornerstone in establishing the reliability of solar energy as a viable and integral part of our energy portfolio.

Fluctuations in energy production, whether due to environmental factors or system inefficiencies, can challenge the seamless integration of solar energy into the power grid [6,7]. To establish the reliability of solar energy as a viable energy source, it is crucial to consider the logistics of stability [8] and variable weather conditions, which can be solved with approaches to accumulate power temporarily—approaches offered by "smart grids". However, regardless of the many ways to avoid grid instability, "the grid operator must sometimes reduce the power generated by other systems (or switch off the PV system) to avoid grid instability" [9].

In the current widely accepted approach, large power generators, such as large coal or hydro power plants, cancel out the oscillations of PV energy fed into the grid by small solar power plants. In some alternative approaches, solar energy is not immediately and directly converted into electrical energy and fed into the electricity grid but is stored by heating rock, water, or something similar to be subsequently converted as indirect solar energy into electricity for electricity distribution.

In the search for stability, the focus is on the stability factor of solar irradiance. This factor summarizes the reliability and consistency of solar irradiance and provides a benchmark for the predictability of energy production. Exploring the intricacies of this stability factor adds another layer to our understanding that helps us develop strategies to improve the reliability of solar energy systems.

In some cases, the stability of solar irradiance in each period, such as a particular day, week, month, or series of months, is particularly interesting. In the literature, we have yet to find a factor that provides this information in a precise and generally acceptable way. Nevertheless, we have found definitions of stability measures for solar irradiance. Stability is usually expressed in terms of the number of sunny days or hours in a time interval [10], but this raises the problem of comparability of defined stability.

This article aims to define the factors (or indexes or parameters) of solar irradiance, separating as far as possible the "nature" of solar electricity production (because of solar irradiance) from the "nature" of solar electricity stability. The proposed factors depend on weather variability and determine the quality of the geographical areas used to produce PV electricity. The determination of irradiance stability is based on historical data, which largely depends on weather and other conditions specific to a given area, providing us with a basis for predicting future solar energy fluctuations. Our factors reach values between 0 and 1, and through repeated observation, different values can be calculated, oscillating between the maximum and minimum factor values for a specific geographical location. All observed values are from one (or a selected) period.

In any case, there is a need to determine the stability of solar irradiance and thus direct electricity generation (as in the case of solar panel use) consistently and comparably. We, therefore, define easily computable stability factors (*SISF*) of solar irradiance, called Solar Irradiance Stability Factors—relative $SISF_r$ as the ratio of the differences between the samples to the samples themselves, $SISF_{am}$ according to the absolute maximum of the observed samples, and $SISF_{dm}$ according to the maximum of the differences between neighboring samples, calculated based on samples of solar irradiance of the horizontal surfaces (e.g., every five minutes) for a given time interval (e.g., one day).

Related Research

In the literature and research, the following basic primary forms of irradiance are primarily mentioned:

1. Direct normal irradiance (*DNI*), or surface shortwave downward radiation or solar irradiance, is defined as the amount of sunlight received from the sun at the surface [11]. It plays a vital role in the dynamics of the earth's surface and drives physical processes in the atmosphere and on the land surface. It is measured at the surface of the earth at a given location with a surface element perpendicular to the sun's direction. It excludes diffuse solar radiation. Direct irradiance is equal to the extraterrestrial irradiance above the atmosphere minus the atmospheric losses due to absorption and scattering [12–15].
2. Diffuse horizontal irradiance (*DHI*) refers to the portion of solar irradiance that reaches a horizontal surface after being scattered by atmospheric particles, clouds, and other obstructions. It is measured on a horizontal surface with radiation from all points in the sky, excluding circumsolar radiation (radiation from the sun disk). *DHI* is essential for understanding solar energy potential, as it contributes significantly to the overall insolation or the total solar radiation energy received on a surface over time. There would be almost no *DHI* in the absence of atmosphere [13,15–18].

3. Global Horizontal Irradiance (*GHI*) is defined as the total solar irradiance received on a horizontal surface, encompassing both diffuse and direct components of solar radiation. It is the sum of *DNI* (after accounting for the solar zenith angle of the sun ζ). *DHI* is represented as $GHI = DHI + DNI \times \cos(\zeta)$ [15,19–21].

In this paper, to calculate *SISF*, we will use samples of solar irradiance, which in our research will be denoted as SI_i. These samples can be *DNI*, *DHI*, *GHI*, or derivatives of these primary forms of irradiance. They can also be measurements outside the earth's atmosphere. The main focus is determining the stability of irradiance, i.e., the differences between individual observed samples. Of course, it is helpful to know more about these samples concerning their nature and measurement method (*DNI*, *DHI*, *GHI*, or something similar), but that is beyond the scope of this paper.

This paper follows some of the already-defined indices that influence our research. The approach developed by Hoff and Perez [22] defines power variability or "Output Variability" as "a measure of the PV Fleet's power output changes over selected sampling Time Interval and analysis period relative to PV Fleet capacity", as shown in the following formula:

$$\sigma_{\Delta t}^{\sum N} = \left(\frac{1}{C^{Fleet}}\right)\sqrt{Var\left[\sum_{n=1}^{N} \Delta P_{\Delta t}^{n}\right]} \tag{1}$$

where C^{Fleet} is the total installed peak power of the fleet and $\Delta P_{\Delta t}^{n}$ is a random variable that represents the time series of changes in power at the nth PV installation using a sampling time interval of Δt [1]. For the purpose of this article, the essence of Equation (1) is that Output Variability is quantified by computing the standard deviation of changes in power output between times t and $t + \Delta t$. If we focus just on the difference between the strength of solar irradiance during a time interval, we see that this approach is like the one defined later in this article. Both approaches are based on the difference between adjacent samples of the PV energy.

However, Hoff and Perez [22] used their Output Variability with their Dispersion Factor to optimize a fleet of PV systems.

In the study of Perez et al. [23], four metrics are defined and used "to quantify short-term variability related to the Hoff and Perez parameter (see Equation (1)), but are dimensionless quantities that remove information about solar geometry and to the size of the considered solar generator, conserving only the information describing variability ($\Delta P_{\Delta t}^{n}$ in Equation (1))". All four metrics are based on the "normalised hourly global horizontal insolation (*GHI*)". Perez et al. [23] defined the hourly global horizontal clear sky index Kt^* as:

$$Kt^* = \frac{GHI}{GHI_{clear}} \tag{2}$$

where "GHI_{clear} represents clear sky global insolation for the considered hour/location". Kt^* is "the ratio of the actual to the clear sky insolation". By analyzing the distribution of the clear sky index over time, we can assess the stability and predictability of solar irradiance. This article, by contrast, defines the factors below, which do not depend on the influence of clear-sky solar irradiance.

In a conference paper, Stein et al. [24] introduced a similar index to Perez et al. [23]. The approach compares the measured solar irradiance and a reference, clear sky solar irradiance, determined from a model. This approach is "the ratio of the length of the measured solar irradiance plotted against time divided by the length of the clear sky solar irradiance plotted against time". It means that "For a clear day, assuming the clear sky model is a perfect match to measurements, Variability Index would be equal to 1, since the sum of the absolute values of the solar irradiance changes would equal the same sum of the clear sky solar irradiance changes" and "extreme overcast of rainy conditions will also have low Variability Index values". The Variability Index is based on the expected energy production (of an ideal clear sky).

The idea developed in this paper was that a measure of stability should be complementary to the measure of the amount of produced energy, and both should be as independent of each other as possible. Expected irradiance depends on geographic location and season, making measures based on this fact harder to compare across different times and geographic areas. Later in this article, three indicators of solar irradiance stability are defined based on the differences between consecutive measured irradiance values rather than on expected irradiance. One characteristic of this approach is that during rainy conditions, we can have very stable irradiance and consequently indicators that show high stability, even though the amount of produced energy in the same observed time interval is very low. The indicators defined in this article are therefore significantly more independent (or orthogonal) from the indicators of produced energy.

The same index—comparison between the measured and clear sky solar irradiance—was also used by Skartveit et al. [25]; Kalogirou et al. [26]; Lave et al. [27]; and Dazhiet et al. [28], among other authors.

Many papers related to the authorship of Badescu [6,7,9,29–31] are based on a "Boolean quantity stating whether the sun is covered or not by clouds" and is used "for the characterization of the radiative regime stability during a given time interval" [7]. The central idea is "Sunshine number" defined as "the sun is shining" at the moment t_j if direct solar irradiance exceeds 120 W/m^2 with the following equation [7]:

$$\xi_{m,j} = \begin{cases} 1;\ if\left(G_j - G_{d,j}\right)/sin(h) > 120\ \mathrm{W/m^2} \\ 0;\ otherwise \end{cases} \quad (3)$$

where the index m denotes "measurement" and h the sun's altitude angle. G and G_d are global and diffuse solar irradiance, respectively.

This metric helps in understanding the temporal variability of solar radiation by providing a simple measure of cloudiness. The Sunshine number can be aggregated over different time periods to understand the frequency and duration of sunny and cloudy periods, which directly impact solar energy availability.

Paulescu and Badescu in Ref. [7] have developed detailed methods for assessing the stability of the solar radiative regime based on "classes of cloud shade, observed total cloud cover amount, daily averaged clearness index, and fractal dimension of the solar global irradiance signal". A clearness index was mentioned above in Perez et al. [23]. In addition, they introduced a "boolean parameter related to solar irradiance fluctuation, namely the Sunshine Stability Number" based on the Sunshine number, which is represented by Equation (3). It considered "the number of changes of Sunshine number that exhibits during a time interval of duration Δt". The combined use of these methods provides a comprehensive framework for assessing the stability of solar irradiance.

Tomson [32] explores the implications of fast-alternating solar radiation on PV systems caused by the movement and alternation of clouds. He utilizes high-resolution irradiance data to capture the fast dynamics of solar radiation. This high-frequency data allows us to calculate the increment of solar global irradiance ΔG in a sequence of recordings $G(t)$. To describe the irradiance time series, a Boolean variable is used. A series has value 1 when $G(t) > G_{aver}$ and 0 when $G(t) < G_{aver}$. G_{aver} is the moving average value of the solar irradiance time series. This paper discusses the importance of energy storage solutions in buffering the effects of fast-alternating solar radiation. Storage systems can smooth out the fluctuations and provide a more consistent power supply, highlighting the need for advanced grid management strategies.

Based on the above-mentioned research and findings, the following sections define indicators of solar irradiance that share some common yet distinctly different characteristics from those previously described. After their concise definition, an extensive discussion follows, presenting their properties along with examples of their application.

2. Methods and Data

In studies of photovoltaic energy storage management and the associated stability of solar radiation, two methods are used simultaneously: qualitative and quantitative. This article's research, conducted using the observation method, is classified as primary research. The presentation of the properties of the proposed solar stability factors with examples of their use is classified as secondary research. The primary research is based on the literature and the observed need for a simple and quick determination of solar radiation stability, which should be as independent as possible from the actual energy production. The secondary research, which presents the proposed factors' use and properties, is based on collected real-world data on solar radiation from various parts of the world with different weather conditions.

Using the proposed factors, information about radiation stability becomes complementary to the amount of energy produced for a specific geographic area. This is crucial for optimizing photovoltaic systems, improving energy storage, enhancing grid integration, and developing predictive models that ensure the reliability and efficiency of solar energy production, which was the primary goal of the research described in this article.

3. Definitions of Solar Irradiance Stability Factors

If we assume as follows:

1. SI_i is the *i*-th sample of solar irradiance;
2. N is the number of samples;
3. $\sum_{i=1}^{N} SI_i > 0$
4. $\Delta SI_i = SI_k - SI_{k+1}$; $k = 1, 2, ..., N-1$ is the difference between two consecutive samples;
5. *F* represents the time frame (for example, from 9:00 to 12:00, which means 3 h);
6. *P* represents the period (length of time) between samples (for example, 1 min).

Then, we define the following three factors:

1. Relative *SISF* is the ratio of the differences between the samples to the samples themselves or the quotient between the oscillating and the total energy. The strict definition is:

$$SISF_r(F,P) = 1 - \frac{max(|\Delta SI_i|) + \sum_{i=1}^{N-1} |\Delta SI_i|}{2 * \sum_{i=1}^{N} |SI_i|} \quad (4)$$

2. Absolute maximum *SISF* is the ratio of the sum of all differences between the consecutive samples to the largest sample. It is an indicator of how big a part oscillations represent according to the largest measured sample. The strict definition is:

$$SISF_{am}(F,P) = 1 - \frac{\sum_{i=1}^{N-1} |\Delta SI_i|}{max(|SI_i|) * (N-1)} \quad (5)$$

3. Difference maximum *SISF* is the ratio of the sum of all differences between the consecutive samples to the largest difference of the consecutive samples. It is an indicator of how much the differences between the samples differ. The strict definition is:

$$SISF_{dm}(F,P) = 1 - \frac{\sum_{i=1}^{N-1} |\Delta SI_i|}{max(|\Delta SI_i|) * (N-1)} \quad (6)$$

All three definitions have the same "nature" of factors based on the differences between neighboring samples, and consequently, the general characteristics of all three are the same. In the following text until the end of this section, the *SISF* is used to treat all three factors ($SISF_r$, $SISF_{am}$, and $SISF_{dm}$).

SISF reaches values between 0 and 1, so a completely (theoretically) stable level of solar irradiance with a factor of 1 is only a hypothetical and theoretical value. This means that the intensity of solar irradiance is constant in the observed time interval—the size of all samples is equal to the maximum sample. In reality, if we observe a more extended time interval (e.g., hours), the scenario with $SISF = 1$ is only observed in the universe or the far north or south of the earth around the summer solstice, when the sun shines evenly throughout the day. In general, such situations are rare on Earth. Figure 1 shows a case where all samples of solar irradiance SI_i in the observed time frame are equal and thus correspond to the maximum value in the observed time frame.

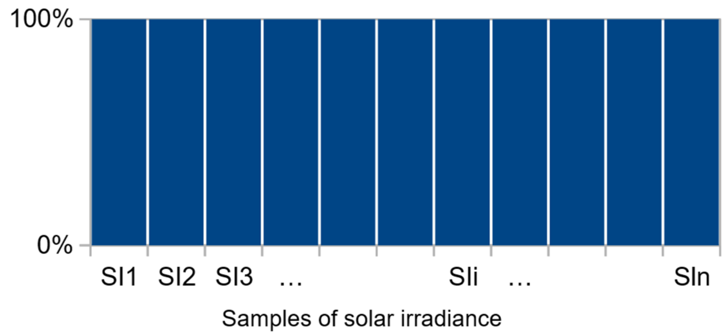

Figure 1. An example of solar irradiance where all samples are equal, greater than 0, and $SRSF = 1$.

On the other hand, the value of $SISF = 0$ is also only hypothetical in practice. In the observed time interval, the samples follow the solar irradiance so that the sun "shines" with its maximum intensity at some points and with its minimum intensity at others. In other words, every second sample corresponds to the maximum sample, while the intermediate samples are identical to the minimum sample. This case is illustrated in Figure 2, where every second sample of solar irradiance SI_i in the observed time frame corresponds to the maximum value, and the others are equal to 0 (or minimum).

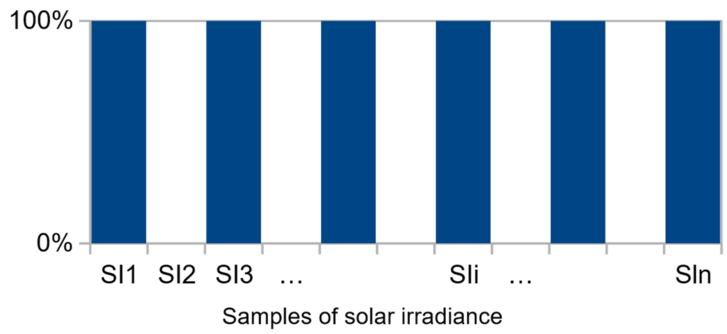

Figure 2. An example of solar irradiance is where samples alternate between a maximum and 0, and $SRSF = 0$.

An essential specification in the *SISF* is the time frame *F*, which was recorded when the *SISF* was calculated. The first parameter in the daily work is a time interval of one day, week, or month. Sampling at equal intervals is the second parameter of the *SISF*. Thus, the *SISF* for samples covering the daily hours of a day and taken every 30 min could be represented as *SISF* (8–17 h, 0.5 h). The calculated *SISF*s are only comparable if the time interval between the samples is the same.

Since the *SISF* complements the factor of average energy produced in a time interval, it would make sense to use both together. Such an approach is used when comparing some of the results in the discussion section.

4. Discussion

4.1. Essence of the SISF

The *SISF*s are based on the difference between two measured samples of solar irradiance and have no direct relation to the theoretical value of solar irradiance under clear skies, even though the observed samples may follow the solar irradiance curve under clear skies. In cloudy weather, when the clouds let little sunshine through, our factors show the stability of the solar irradiance—although the solar irradiance is much lower than in clear skies. On the other hand, the *SISF*s show slightly worse stability under clear skies than under stable cloudy weather, as the differences between the two samples are more considerable when the sun rises or sinks towards the horizon, as shown in Figure 3. It shows that delta1 is larger than delta2, so the *SISF*s are less stable under clear skies than cloudy skies.

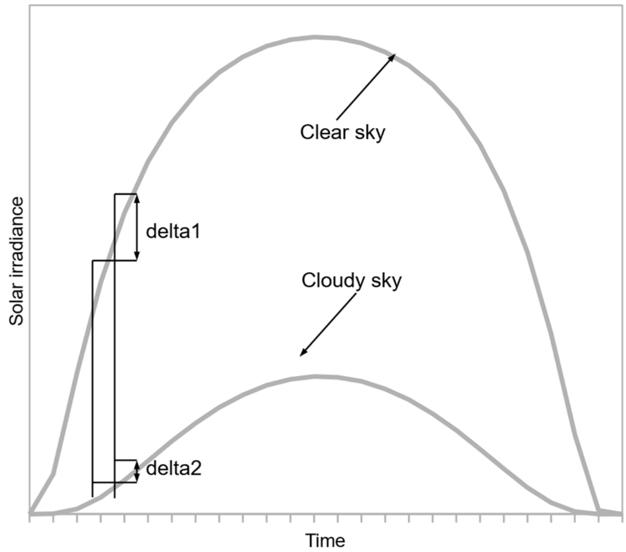

Figure 3. Solar irradiance in clear (with lower stability) and cloudy (with higher stability) sky conditions with more extensive and smaller differences between solar irradiance size samples. Source: Ref. [33].

There is a similarity between the Badescu and Tomson approach mentioned above and our approach for observing and comparing successive solar irradiance values. However, the definitions of the values that allow us to make comparisons between the individual measurements are different, and consequently, so is the nature of the values.

4.2. Example 1 of SISF Calculation

We assume that the data on solar irradiance is available on January, April, July, and October 1st of each year. In our case, the data was obtained from the Environmental Agency of Slovenia. Solar irradiance was measured in the center of Ljubljana (about 46 degrees north latitude) and represents samples of solar irradiance on horizontal surfaces in (W/m^2). The measurements were taken every half hour. The graph in Figure 4 is a graphical representation of solar irradiance. Figure 4 shows the so-called “clear sky” effect on 1 January and 1 July. For both months, it is not unusual for a “clear sky” to be present at this geographic latitude.

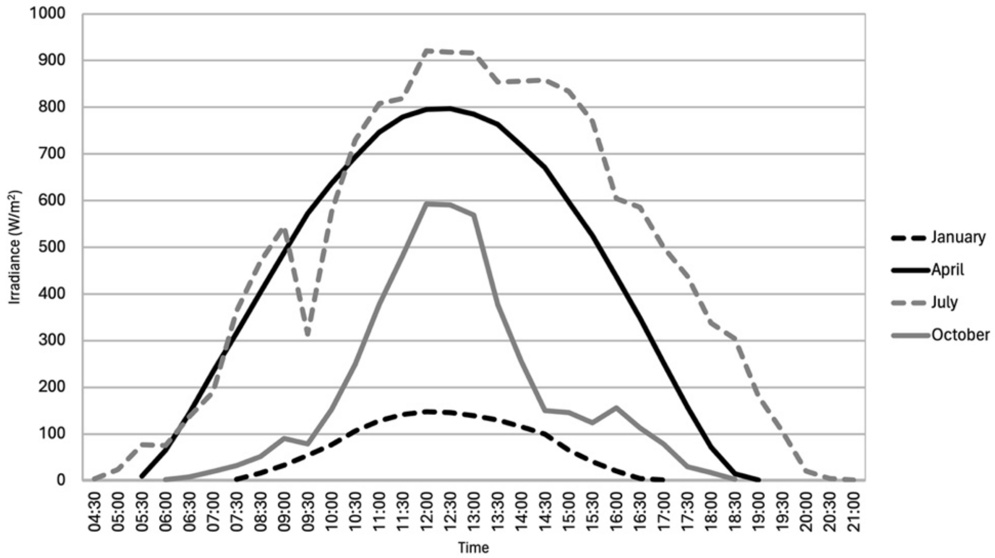

Figure 4. Solar irradiance distribution on 1 January, 1 April, 1 July, and 1 October in Ljubljana (with a latitude of about 46° north) in the same year. Source: Ref. [33].

Table 1 contains the data for 1 January, as shown in the graph in Figure 4. These data refer to the time interval, the sample size, and the absolute difference between the two samples.

Table 1. Time intervals; samples of solar irradiance on 1 January in Ljubljana, as shown in Figure 4; and their absolute differences. Source: own elaboration.

	SI_i (W/m^2)	$\lvert\Delta SI_i\rvert = \lvert SI_k - SI_{k+1}\rvert$ (W/m^2)
08:00	3	
08:30	16	13
09:00	33	17
09:30	54	21
10:00	77	23
10:30	106	29
11:00	128	22
11:30	142	14
12:00	148	6
12:30	146	2
13:00	139	7
13:30	130	9
14:00	116	14
14:30	100	16
15:00	65	35
15:30	41	24
16:00	21	20
16:30	5	16
17:00	1	4

Using the data in Table 1, we calculated $SISF_{am}$ as one of the $SISF$s as follows:

- $max(\Delta SI_i) = 35\ \mathrm{W/m^2}$
- $N = 19$
- $\sum_{i=1}^{N-1} \lvert\Delta SI_i\rvert = 292\ \mathrm{W/m^2}$
- $SISF_{am}\ (8\text{–}17\ \mathrm{h}, 0.5\ \mathrm{h}) = 1 - \frac{\sum_{i=1}^{N-1} \lvert\Delta SI_i\rvert}{max(SI_i) * (N-1)} = 0.8904$

The calculated total energy of the day is the sum of the solar irradiance values observed every 30 min. Therefore, the day's total energy is 735.5 Wh/m^2 over a horizontal surface. Solar panels that are usually directed towards the sun would receive more energy.

Other values for *SISF*s (8–17 h, 0.5 h) and the energy received in the same time interval are listed below in Table 2 (see also Figure 4).

Table 2. Calculated $SISF_r$, $SISF_{am}$, $SISF_{dm}$, and the energy received in a day in Ljubljana during different seasons of the same year. Source: Ref. [33].

Date	$SISF_r$ (8–17 h, 0.5 h)	$SISF_{am}$ (8–17 h, 0.5 h)	$SISF_{dm}$ (8–17 h, 0.5 h)	$\sum_{i=1}^{N-1}(SI_i * 0.5)$(Wh/m^2)
1 January	0.7777	0.8904	0.5365	735
1 April	0.9011	0.9286	0.4074	6012
1 July	0.8709	0.9127	0.6930	7571
1 October	0.6926	0.9110	0.7250	2373

4.3. Example 2 of SISF Calculation

So far, we have calculated the $SISF_{am}(24\,\text{h}, 0.5\,\text{h})$ values (with 24 h, we cover all samples greater than 0) for each whole month. We have observed January, April, July, and October of the same year. $SISF_{am}(24\,\text{h}, 0.5\,\text{h})$ can be calculated daily, and its value can be examined within a month. The graphs for the months are shown in Figure 5. The mean values and standard deviations of $SISF_{am}(24\,\text{h}, 0.5\,\text{h})$ and the amount of energy received per month are shown in Table 3. Such graphs (see Figure 5) are useful for quickly assessing the dispersion of solar irradiance stability and the quantity of energy produced for a specific geographical area by individual months (the observed time period could also differ).

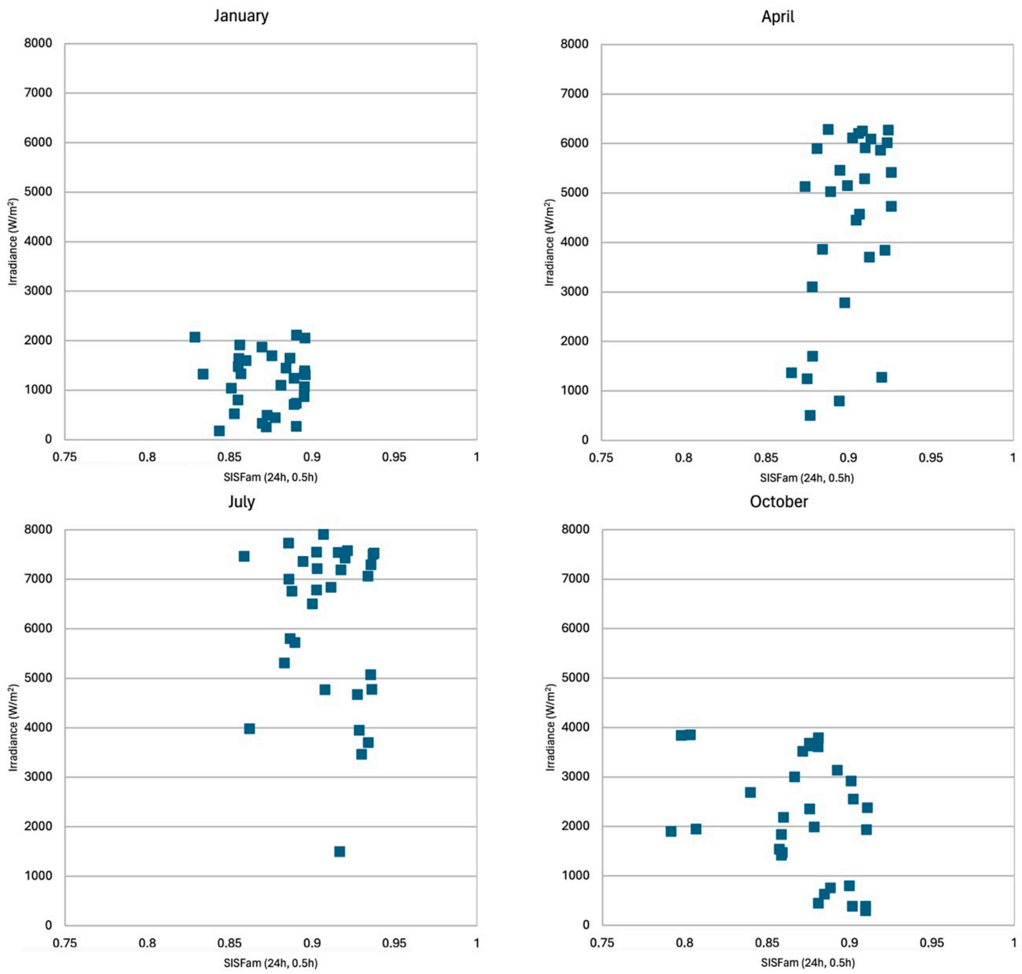

Figure 5. Daily distribution of $SISF_{am}$ and solar energy in Ljubljana for January, April, July, and October of a year. Source: own elaboration.

Table 3. Mean values and standard deviations of $SISF_{am}$ per month in Ljubljana. Source: own elaboration.

Month	Average	Std Dev	Energy (kWh/m^2)
January	0.87	0.02	36
April	0.90	0.02	130
July	0.91	0.02	191
October	0.87	0.03	65

4.4. Example 3 of SISF Calculation

Figure 6 shows three daily distributions of solar irradiance in Ljubljana for the month of July. The distributions are obviously different. Table 4 shows the corresponding three *SISF*s.

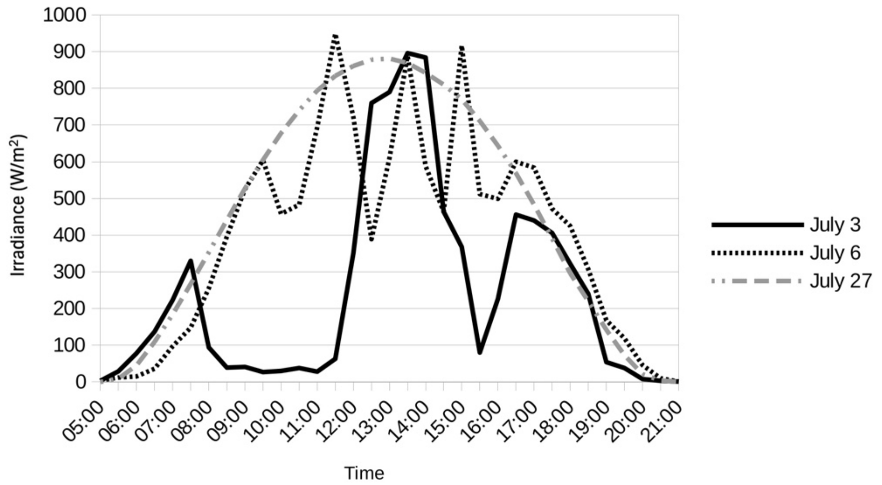

Figure 6. Daily distributions of solar irradiance in Ljubljana for 3, 6, and 27 July in a year. Source: Ref. [33].

Table 4. Calculated *SISF*s for the daily distribution of solar irradiance from Figure 6. Source: Ref. [33].

	$SISF_r$ (5–21 h, 0.5 h)	$SISF_{am}$ (5–21 h, 0.5 h)	$SISF_{dm}$ (5–21 h, 0.5 h)
3 July	0.77423	0.88594	0.75668
6 July	0.81750	0.85870	0.70399
27 July	0.93874	0.93383	0.38632

$SISF_r$ is smallest on 3 July, followed by 6 July, and has the highest value on 27 July, as can be seen in Figure 6.

$SISF_{am}$ has the lowest value on 6 July and is slightly larger on 3 July. In Figure 6, we see that the length of the lines representing the oscillation of solar irradiance (especially between 10:00 and 17:00) is slightly greater on 6 July than on 3 July. This means that the sum of the oscillation lengths is slightly greater on 6 July than on 3 July, while the maximum patterns are similar in both cases. 27 July has the best value of $SISF_{am}$, as the differences between samples are relatively small. The stability factor $SISF_{am}$ on 27 July is not close to 1, contrary to what would be expected for factors defined based on the difference between the observed solar irradiance and the open sky irradiance in this particular "near open sky" solar irradiance curve.

Figure 3 represents the situation when all differences between the samples are equal. This means that $SISF_{dm} = 0$. $SISF_{dm}$ focuses only on the difference between the samples, regardless of how these differences are shifted from the abscissa in our graphs (see Figure 6), and in our case, the differences between the samples are smallest on 27 July and $SISF_{dm}$ has the smallest value of our three samples according to the definition (see Equation (5)).

4.5. Example 4 of SISF Calculation

In the following example, all three *SISF*s are shown using data from Bahrain and Slovenia (Gačnik, a few kilometers from Maribor, with continental climate conditions). The intervals between measurements are 5 min (300 s), and a day is divided into four equivalent 3 h time windows starting at 6:00, 9:00, 12:00, and 15:00. The solar irradiance during each of these time windows is shown in Figure 7.

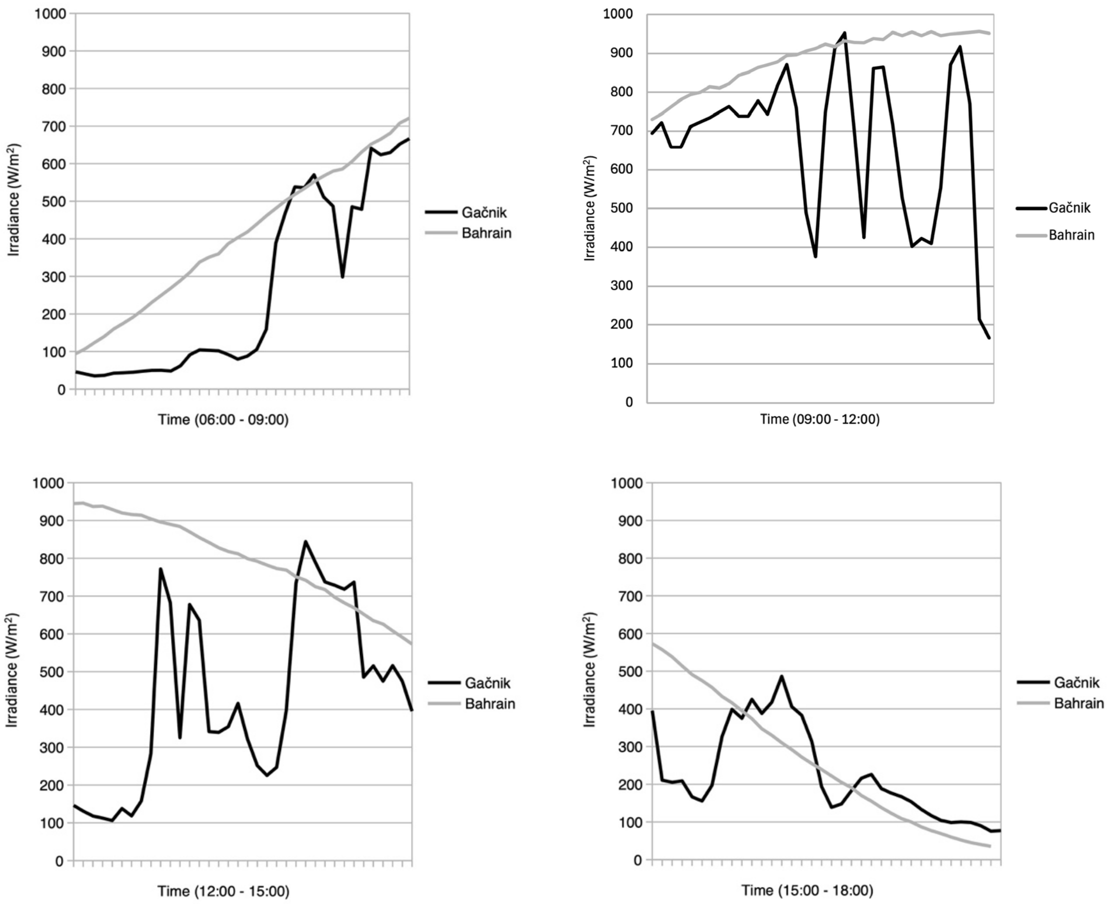

Figure 7. Solar irradiance distribution during one day in Bahrain and Gačnik in four different periods. Source: own elaboration.

As we can see from the graphs, the distribution of solar irradiance in Bahrain is much more stable and predictable than in Gačnik; and the expected values for the *SISF*s should reflect this fact.

The calculated values for all three *SISF*s for Bahrain and Gačnik are shown in Tables 5 and 6, respectively.

Table 5. Bahrain-calculated *SISF*s based on the data represented in Figure 7 for different time frames with the 5 min distance between samples. Source: own elaboration.

t	$SISF_r\ (t, 300\ \text{s})$	$SISF_{am}\ (t, 300\ \text{s})$	$SISF_{dm}\ (t, 300\ \text{s})$
06:00–09:00	0.97774	0.97515	0.33651
09:00–12:00	0.99465	0.99045	0.58442
12:00–15:00	0.99308	0.98864	0.46286
15:00–18:00	0.96798	0.97160	0.41414

Table 6. Gačnik-calculated *SISF*s based on the data represented in Figure 7 for different time frames with 5 min distance between samples. Source: own elaboration.

t	$SISF_r\ (t, 300\ \text{s})$	$SISF_{am}\ (t, 300\ \text{s})$	$SISF_{dm}\ (t, 300\ \text{s})$
06:00–09:00	0.91953	0.94466	0.83955
09:00–12:00	0.90119	0.87349	0.7838
12:00–15:00	0.87429	0.88510	0.80145
15:00–18:00	0.92037	0.93446	0.75258

The value $SISF_r$, which represents the relative ratio between the sample differences and the samples themselves, is high in the case of Bahrain and lower in the case of Gačnik, as expected. In Bahrain, the solar irradiance curve is steeper in the first and last time frames than in the second and third time frames, and consequently, the stability factor $SISF_r$ is slightly smaller in the first and last time frames than in the second and third time frames. In Gačnik, the second and especially the third time frames are unstable, as shown in Figure 7. However, the oscillation frequency of the solar irradiance is relatively low, which is why the factor is still relatively high. The higher the frequency, the lower the stability and the smaller the factor.

$SISF_{am}$ and $SISF_{dm}$ should be considered together. They are similar; the first represents the ratio between the average sample and the largest sample in the observed time interval, while the second represents the ratio between the average sample and the largest difference between the samples. In the case of Bahrain, $SISF_{am}$ is relatively high and comparable to $SISF_r$, while $SISF_{dm}$ is relatively small compared to $SISF_{am}$. Such a situation represents the case of stable solar irradiance with small differences between samples. This small difference between the samples leads to a high sensitivity of $SISF_{dm}$.

4.6. Example 5 of SISF Calculation

The following presents Gačnik on 2 May 2015, in the time interval between 12:00 and 15:00, with sampling every 10 s. Then, the average of all six consecutive samples was converted to sampling every 60 s (1 min), and the average of all 30 consecutive samples was converted to sampling every 300 s (5 min).

The number of time samples in the same period leads to different *SISF* results. This consequence is due to the following:

1. By averaging the solar irradiance during a time sample, many peaks in solar irradiance are smoothed out, as shown in Figure 8—a larger time frame smooths out more energy peaks that may occur. As a result, a more stable irradiance is observed;
2. We have more samples within a given observed time interval with a decrease in the time difference between the samples. The number of these samples is represented in Table 7 in the column labeled '$N-1$'. As their number increases, the values of *SISF*s converge towards 1, which arises from the definition of *SISF* itself.

Table 7. Gačnik-calculated SISF based on solar irradiance using different (10, 60, and 300 s) time samples shown in Figure 8. Source: own elaboration.

F	$N-1$	$SISF_r(P,F)$	$SISF_{am}(P,F)$	$SISF_{dm}(P,F)$
10 s	1079	0.97651	0.98260	0.97287
60 s	189	0.94336	0.95439	0.90085
300 s	36	0.87429	0.88510	0.80145

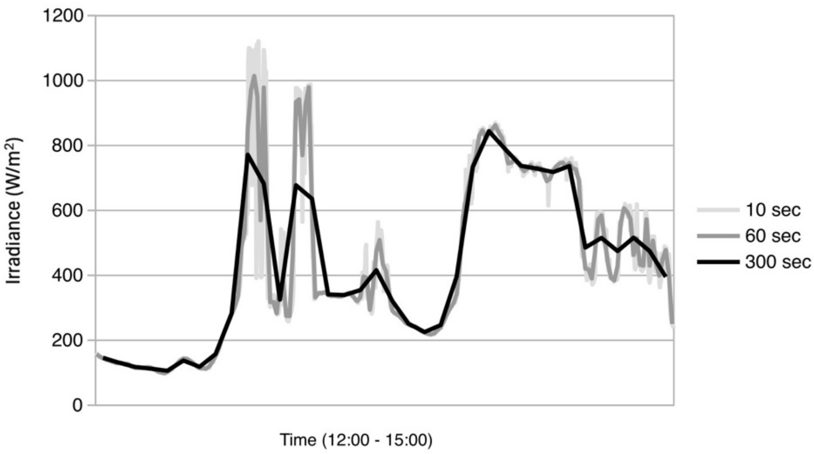

Figure 8. Representation of solar irradiance using different (10, 60, and 300 s) time samples. Source: own elaboration.

For these reasons, we must compare the *SISF* with the same time differences between the samples; otherwise, the *SISF*s are not comparable.

However, the extent of the periods that should be used in practice differs from this article's topic.

5. Conclusions

Beyond quantity, the stability of PV energy is a critical factor in our quest for a reliable and consistent energy supply. The inherent variability of solar energy production requires a paradigm shift in how we approach energy stability. By addressing the logistics of stability, our findings contribute to the field of renewable energy and the broader discourse on securing a resilient and sustainable energy future.

Solar Irradiance Stability Factors (*SISF*s) are proving to be critical metrics for understanding and characterizing the stability of solar irradiance for specific locations. These factors are calculated based on historical sample values for solar irradiance intensity and provide insight into the fluctuations influenced by weather conditions, atmospheric particles such as PMx, and other contextual elements that affect solar radiation. The oscillation between maximum and minimum factor values and the calculations of mean and standard deviation allow for a nuanced investigation of the stability of solar irradiance.

The temporal classification of these factors opens possibilities for comparative analyses, whether within a specific month, over different years, or for selected days. When these factors are compared to energy production values for the same time intervals, our understanding of the suitability of a geographic area for solar energy production improves. This analysis is particularly crucial in regions where weather conditions fluctuate significantly from hour to hour, day to day, or week to week, such as in Slovenia, as shown in Example 4 of the *SISF* calculation. In such areas, the variability of solar irradiance plays a pivotal role in energy planning and logistics. Conversely, in regions like Bahrain, where weather conditions are expected to remain stable and predictable day after day, the utility of these factors is less pronounced, as the consistency of solar irradiance simplifies energy production forecasting and reduces the need for detailed variability analysis. *SISF*s were initially developed with power generation needs and characteristics in mind, but their versatility extends to general solar irradiance information.

A promising way forward is the development of maps showing areas of stable solar irradiance. Based on historical data for different periods and months, these maps could complement existing solar energy production maps and thus contribute to better site selection and planning. The planned on-the-fly computations based on interactive data have the potential to provide real-time insights, especially when combined with radar maps of the clouds, their expected direction, and other relevant data. Such comprehensive information dissemination is a vital prerequisite for early and informed decision-making, particularly in industries such as smart grids.

While this article examines the behavior of solar irradiance over a year at a specific location, it prompts consideration of a broader perspective. Future studies should encompass locations worldwide, each characterized by unique meteorological conditions that significantly influence the logistics of solar energy production, including those related to photovoltaic (PV) or wind energy. This expanded comparative analysis will validate the utility of Solar Irradiance Stability Factors (*SISF*s) as valuable information and enhance decision-making processes in selecting optimal sites for solar power generation and other relevant applications.

Funding: This research received no external funding.

Data Availability Statement: Dataset available on request from the authors.

Conflicts of Interest: The authors declare no conflict of interest.

References

1. Eurostat Electrical Capacity for Wind and Solar Photovoltaic Power—Statistics. Available online: https://ec.europa.eu/eurostat/statistics-explained/index.php?title=Electrical_capacity_for_wind_and_solar_photovoltaic_power_-_statistics (accessed on 2 May 2024).
2. President, T.S. Preparing the Grid for Renewable Energy: Electric Warehouses. Available online: https://www.prescientelectric.com/post/preparing-the-grid-for-renewable-energy-electric-warehouses (accessed on 2 May 2024).
3. Kim, K.A.; Bagci, F.S.; Dorsey, K.L. Design Considerations for Photovoltaic Energy Harvesting in Wearable Devices. *Sci. Rep.* **2022**, *12*, 18143. [CrossRef]
4. Mellit, A.; Pavan, A.M. A 24-h Forecast of Solar Irradiance Using Artificial Neural Network: Application for Performance Prediction of a Grid-Connected PV Plant at Trieste, Italy. *Sol. Energy* **2010**, *84*, 807–821. [CrossRef]
5. Bădescu, V. *Modeling Solar Radiation at the Earth's Surface: Recent Advances*; Springer: Berlin/Heidelberg, Germany, 2008; ISBN 978-3-540-77454-9.
6. Badescu, V.; Abed, Q.A.; Ciocanea, A.; Soriga, I. The Stability of the Radiative Regime Does Influence the Daily Performance of Solar Air Heaters. *Renew. Energy* **2017**, *107*, 403–416. [CrossRef]
7. Paulescu, M.; Badescu, V. New Approach to Measure the Stability of the Solar Radiative Regime. *Theor. Appl. Climatol.* **2011**, *103*, 459–470. [CrossRef]
8. Mahela, O.P.; Shaik, A.G. Power Quality Recognition in Distribution System with Solar Energy Penetration Using S-Transform and Fuzzy C-Means Clustering. *Renew. Energy* **2017**, *106*, 37–51. [CrossRef]
9. Badescu, V.; Budea, S. How Significant Is the Stability of the Radiative Regime When the Best Operation of Solar DHW Systems Is Evaluated? *Renew. Energy* **2016**, *88*, 346–358. [CrossRef]
10. Knez, M.; Jereb, B. Solar Power Plants—Alternative Sustainable Approach to Greener Environment: A Case of Slovenia. *Sustain. Cities Soc.* **2013**, *6*, 27–32. [CrossRef]
11. Huang, G.; Li, Z.; Li, X.; Liang, S.; Yang, K.; Wang, D.; Zhang, Y. Estimating Surface Solar Irradiance from Satellites: Past, Present, and Future Perspectives. *Remote Sens. Environ.* **2019**, *233*, 111371. [CrossRef]
12. Rodríguez, E.; Cornejo-Ponce, L.; Cardemil, J.M.; Starke, A.R.; Droguett, E.L. Estimation of One-Minute Direct Normal Irradiance Using a Deep Neural Network for Five Climate Zones. *Renew. Sustain. Energy Rev.* **2023**, *183*, 113486. [CrossRef]
13. Schlager, E.; Feichtinger, G.; Gursch, H. Development and Comparison of Local Solar Split Models on the Example of Central Europe. *Energy AI* **2023**, *12*, 100226. [CrossRef]
14. Abreu, E.F.M.; Canhoto, P.; Costa, M.J. Prediction of Circumsolar Irradiance and Its Impact on CSP Systems under Clear Skies. *Energies* **2023**, *16*, 7950. [CrossRef]
15. Overen, O.K.; Meyer, E.L. Solar Energy Resources and Photovoltaic Power Potential of an Underutilised Region: A Case of Alice, South Africa. *Energies* **2022**, *15*, 4646. [CrossRef]
16. Abreu, E.F.M.; Canhoto, P.; Costa, M.J. Prediction of Diffuse Horizontal Irradiance Using a New Climate Zone Model. *Renew. Sustain. Energy Rev.* **2019**, *110*, 28–42. [CrossRef]
17. Kotti, M.C.; Argiriou, A.A.; Kazantzidis, A. Estimation of Direct Normal Irradiance from Measured Global and Corrected Diffuse Horizontal Irradiance. *Energy* **2014**, *70*, 382–392. [CrossRef]
18. Hofmann, M.; Seckmeyer, G. A New Model for Estimating the Diffuse Fraction of Solar Irradiance for Photovoltaic System Simulations. *Energies* **2017**, *10*, 248. [CrossRef]
19. Olmo, F.J.; Vida, J.; Foyo, I.; Castro-Diez, Y.; Alados-Arboledas, L. Prediction of Global Irradiance on Inclined Surfaces from Horizontal Global Irradiance. *Energy* **1999**, *24*, 689–704. [CrossRef]
20. Awan, A.B.; Zubair, M.; Chandra Mouli, K.V.V. Design, Optimization and Performance Comparison of Solar Tower and Photovoltaic Power Plants. *Energy* **2020**, *199*, 117450. [CrossRef]

21. Sawadogo, W.; Bliefernicht, J.; Fersch, B.; Salack, S.; Guug, S.; Diallo, B.; Ogunjobi, K.; Nakoulma, G.; Tanu, M.; Meilinger, S.; et al. Hourly Global Horizontal Irradiance over West Africa: A Case Study of One-Year Satellite- and Reanalysis-Derived Estimates vs. in Situ Measurements. *Renew. Energy* **2023**, *216*, 119066. [CrossRef]
22. Hoff, T.E.; Perez, R. Quantifying PV Power Output Variability. *Sol. Energy* **2010**, *84*, 1782–1793. [CrossRef]
23. Perez, R.; Kivalov, S.; Schlemmer, J.; Hemker, K.; Hoff, T. Parameterization of Site-Specific Short-Term Irradiance Variability. *Sol. Energy* **2011**, *85*, 1343–1353. [CrossRef]
24. Stein, J.; Hansen, C.; Reno, M. The Variability Index: A New and Novel Metric for Quantifying Irradiance and PV Output Variability. In *Proceedings of the World Renewable Energy Congress*; Curran: Red Hook, NY, USA, 2012; Volume 2012.
25. Kalogirou, S.A.; Pashiardis, S.; Pashiardi, A. Statistical Analysis and Inter-Comparison of the Global Solar Radiation at Two Sites in Cyprus. *Renew. Energy* **2017**, *101*, 1102–1123. [CrossRef]
26. Skartveit, A.; Olseth, J.A.; Tuft, M.E. An Hourly Diffuse Fraction Model with Correction for Variability and Surface Albedo. *Sol. Energy* **1998**, *63*, 173–183. [CrossRef]
27. Lave, M.; Reno, M.J.; Broderick, R.J. Characterizing Local High-Frequency Solar Variability and Its Impact to Distribution Studies. *Sol. Energy* **2015**, *118*, 327–337. [CrossRef]
28. Dazhi, Y.; Jirutitijaroen, P.; Walsh, W.M. The Estimation of Clear Sky Global Horizontal Irradiance at the Equator. *Energy Procedia* **2012**, *25*, 141–148. [CrossRef]
29. Brabec, M.; Badescu, V.; Paulescu, M. Nowcasting Sunshine Number Using Logistic Modeling. *Meteorol. Atmos. Phys.* **2013**, *120*, 61–71. [CrossRef]
30. Paulescu, M.; Badescu, V.; Brabec, M. Tools for PV (Photovoltaic) Plant Operators: Nowcasting of Passing Clouds. *Energy* **2013**, *54*, 104–112. [CrossRef]
31. Soriga, I.; Badescu, V. Performance of SDHW Systems with Fully Mixed and Stratified Tank Operation under Radiative Regimes with Different Degree of Stability. *Energy* **2017**, *118*, 1018–1034. [CrossRef]
32. Tomson, T. Fast Dynamic Processes of Solar Radiation. *Sol. Energy* **2010**, *84*, 318–323. [CrossRef]
33. Jereb, B. Stability of Solar Radiation as an Important PV Energy Quality Parameter. In Proceedings of the SOLARIS Conference 2017, London, UK, 27–28 July 2017. [CrossRef]